

Synthesis of CZTS Nanoparticles for Low-Cost Solar Cells

Donguk Kim¹, Minha Kim¹, Joongpyo Shim², Doyoung Kim³, Wonseok Choi⁴,
Yong Seob Park⁵, Youngkwan Choi⁶, and Jaehyeong Lee^{1,*}

¹*School of Electronic and Electrical Engineering, Sungkyunkwan University, Suwon, 440-746, Republic of Korea*

²*Department of Nano and Chemical Engineering, Kunsan National University, Kunsan, 573-701, Republic of Korea*

³*School of Electrical and Electronic Engineering, Ulsan College, Ulsan, 680-749, Republic of Korea*

⁴*Department of Electrical Engineering, Hanbat National University, Daejeon, 305-719, Republic of Korea*

⁵*Department of Photoelectronics, Chosun College of Science and Technology, Gwangju 501-744, Republic of Korea*

⁶*Water Facility Research Center, K-Water, Daejeon, 305-730, Republic of Korea*

In this work, uniformly sized $\text{Cu}_2\text{ZnSnS}_4$ (CZTS) nanoparticles with easy control of chemical composition were synthesized and printable ink containing CZTS nanoparticles was prepared for low-cost solar cell applications. In addition, we studied the effects of synthesis conditions, such as reaction temperature and time, on properties of the CZTS nanoparticles. For CZTS nanoparticles synthesis process, the reactants were mixed as the 2:1:1:4 molar ratios. The reaction temperature and time was varied from 220 °C to 320 °C and from 3 hours to 5 hours, respectively. The crystal structure and morphology of CZTS nanoparticles prepared under the various conditions were investigated by X-ray diffraction (XRD) and field-emission scanning electron microscopy (FE-SEM), and energy dispersive X-ray spectroscopy (EDS) was used for compositional analysis of the CZTS nanoparticles.

Keywords: $\text{Cu}_2\text{ZnSnS}_4$ (CZTS), Nanoparticles, Synthesis, Solar Cells.

1. INTRODUCTION

In the PV industry, a lot of solar cell companies have reduced solar power cost toward the current conventional cost of electricity. For low-cost solar cell, among the various compound semiconductors, the I–III–VI₂ family of chalcogenide as CuInSe_2 (CIS), CuGaSe_2 (CGS), $\text{Cu}(\text{In}_x\text{Ga}_{1-x})(\text{S}_y\text{Se}_{1-y})_2$ (CIGS) have been developed as thin film solar cell. Today, the laboratory CIGS solar cell with small size has led to the highest efficiency of over 20% in the chalcogenide thin film solar cell,¹ and CIGS modules have been successfully produced on an industrial large scale.^{2–4} However, due to relatively expensive and scarce materials as In and Ga, the CIGS solar cell has been still issues of long term sustainability in terms of cost and availability.⁵

For these days, the *p*-type quaternary compound $\text{Cu}_2\text{ZnSnS}_4$ (CZTS) have been investigated as new material, which is nontoxic, earth-abundant and cheap. The CZTS structure is tetragonal and could be obtained by

replacing In(III) of the chalcopyrite CIS structure by Zn(II) and Sn(IV) in a 50:50 ratio.^{5,6} The bandgap of CZTS was reported as the direct bandgap of 1.45 eV,⁷ which is close to the optimum direct band gap value for single junction solar cell.⁸ The absorption coefficient of CZTS was investigated in the order of 10^4 cm^{-1} near a fundamental absorption edge,^{9,10} which is similar to about 10^5 cm^{-1} of CIGS.¹¹ Thanks to these good properties, CZTS has been expected as a promising candidate for low cost absorber layers.

Today, the highest performance of CZTS based solar cells are 8.4% for pure sulfur CZTS absorber deposited by vacuum thermal evaporation process,¹² and 12.6% for CZTS absorber with S and Se coated by an ink made by hydrazine solution.¹³ There have been various high vacuum such as sputtering, evaporation and non-vacuum such as solution(ink), electrode deposition, for the deposition of CZTS thin films.¹⁴

Here, we report the CZTS synthesis of nanopowder that will be dispersed in an ink by the method referred to as Steinhagen et al.¹⁵ In this work, uniformly sized

*Author to whom correspondence should be addressed.

Table I. Synthesis conditions for CZTS nanoparticles.

Chemicals	MW	Mmol	Weight (g)	Atomic ratio
Cu(II) acetylacetonate	261.76	2.275	0.5956	2.00
Zinc acetylacetonate hydrate	281.62	1.138	0.3204	1.00
Tin(IV) bis(acetylacetonate) dibromide	476.73	1.138	0.5424	1.00
Sulfur	32.07	4.549	0.1459	4.00

Cu₂ZnSnS₄ (CZTS) nanoparticles with easy control of chemical composition were synthesized and printable ink containing CZTS nanoparticles was prepared for low-cost solar cell applications. In addition, we studied the effects of synthesis conditions, such as reaction temperature and time, on properties of the CZTS nanoparticles.

2. EXPERIMENTAL DETAILS

CZTS nanoparticles were synthesized at different temperatures (220–320 °C) for 3 hours and for various reaction times (2–5 hours) at 240 °C, using high-temperature arrested precipitation in the coordinating solvent, oleylamine (OLA).¹⁵ Under the reaction time of 3 hours, the reactants for synthesis of CZTS nanoparticles didn't dissolve enough in OLA. Copper(II) acetylacetonate (>99.99%, from Sigma-Aldrich), zinc acetylacetonate (from DONGSAN Chemical Co.) tin(IV) bis(acetylacetonate) dibromide (97%, from Sigma-Aldrich) and elemental sulfur (80%, from Sigma-Aldrich) (as shown in Table I) were put in 100 mL OLA (70%, from

Sigma-Aldrich) in 1 liter five-neck flask, and heated to the different temperature with magnetic stirrer under an inert atmosphere made by nitrogen purging for enough time, instead of Schlenk line. To prevent mass-loss during reaction, Liebig condenser to circulate water was set up on the flask. At the different temperature, the mixture was reacted for the various time. After the CZTS synthesis, the reacted mixture was cooled to room temperature. In addition, 100 mL Hexane (95%, from DAEJUNG CHEMICALS AND METALS Co.) was put in the flask, and the reacted mixture was stirred for 1 hour to remove solid reaction byproducts and poorly capped nanocrystals by redispersion of hexane.^{15,16} The reacted mixture was equally divided by six 50 mL conical tubes, then some amount of ethanol (99.9%, from SAMCHUN PURE CHEMICALS Co.) was added in considering weight balance for centrifugation and to clean the CZTS nanoparticles from OLA. CZTS nanocrystals were obtained, using centrifugation at 8000 rpm for 10 minutes for isolation of CZTS nanocrystals from the mixtures. The obtained CZTS nanocrystals were washed five more times by solvent/antisolvent precipitation with

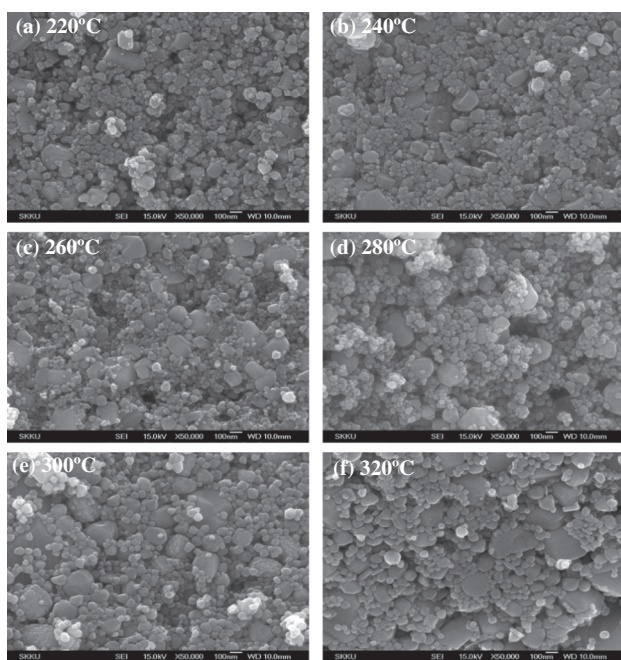


Figure 1. SEM images of the CZTS nanoparticles synthesis at different temperatures: (a) 220 °C, (b) 240 °C, (c) 260 °C, (d) 280 °C, (e) 300 °C, (f) 320 °C. The reaction time was 3 hours.

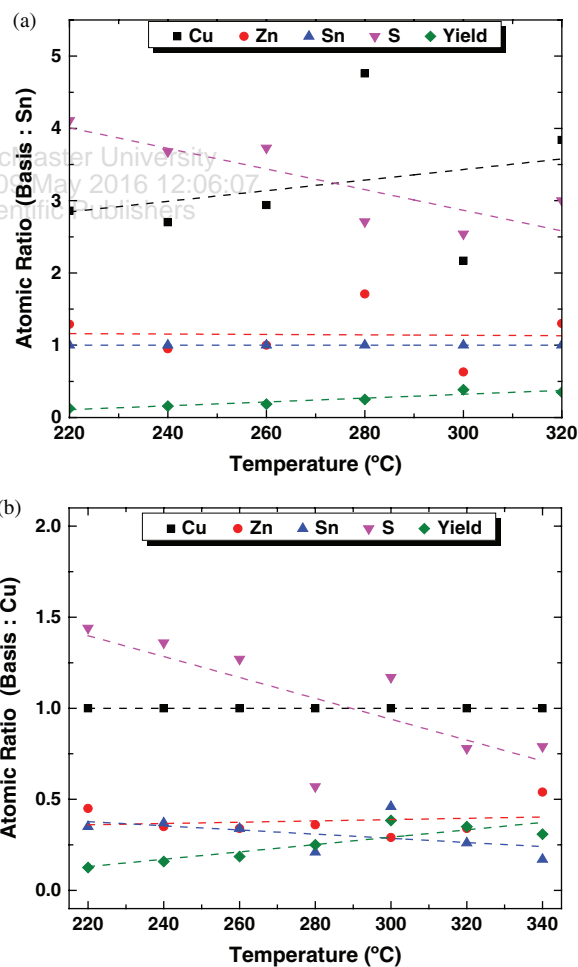


Figure 2. EDS analysis of CZTS nanoparticles prepared at different temperatures (a) when Sn ratio is fixed to a reference (Sn = 1) and (b) when when Sn ratio is fixed to a reference (Cu = 1).

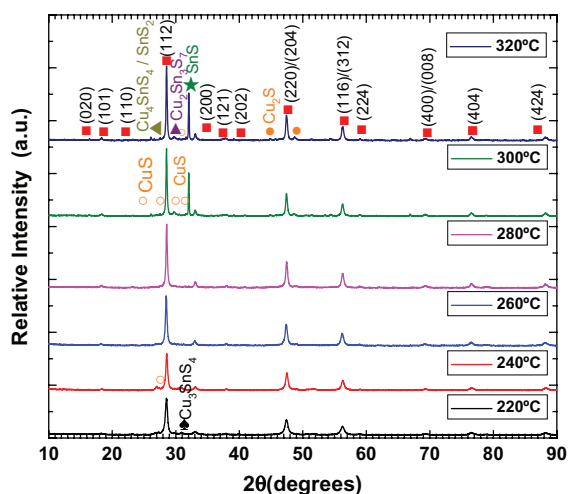


Figure 3. XRD patterns of the CZTS nanoparticles synthesized at different temperatures.

hexane/ethanol.^{15,16} The slurry of the CZTS nanocrystals was dried in vacuum dry oven at 100 °C to get CZTS nanopowder. The CZTS ink was made by sonification of 1 mL hexanethiol (95%, from Sigma-Aldrich) with the CZTS nanoparticles for dispersion. The CZTS ink was printed directly onto soda lime glass by blade coating. After the blade coating, the film was dried in the vacuum oven at 150 °C for 15 min.

3. RESULTS AND DISCUSSION

Figure 1 shows SEM images of the CZTS nanoparticles synthesized at different temperatures. When the reaction temperature was elevated, the particle size increased. In addition, some large particles appeared as the synthesis temperature increased. In particular, non-uniform and large CZTS nanoparticles were exhibited at higher temperature than 260 °C. Therefore, the synthesis temperature should

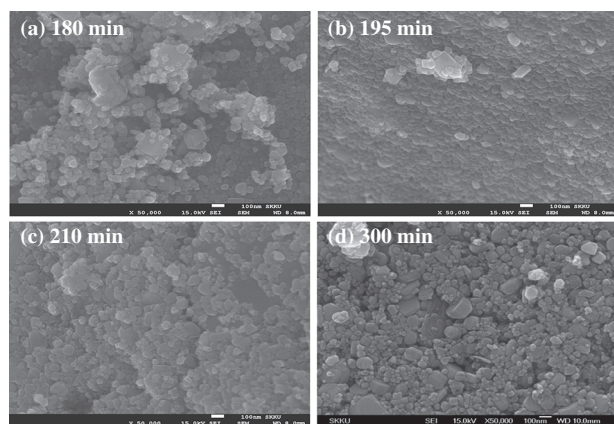


Figure 4. SEM images of the CZTS nanoparticles synthesized for various times: (a) 180 min, (b) 195 min, (c) 210 min, (d) 300 min. The reaction temperature was 3 hours.

be under 260 °C for synthesis of uniformly sized CZTS nanoparticles.

Figure 2 shows EDS analysis of CZTS nanoparticles prepared at different temperatures. As the synthesis temperature increased, a stoichiometry of CZTS nanoparticles became Cu rich and S poor due to Sn and chalcogen loss during reaction.^{17,18} When Cu ratio is fixed to a reference (Fig. 2(b)), S amount decreased sharply and Sn ratio was slightly reduced with the reaction temperature. All the reactants was put into the flask at once for synthesis, so the compositional variation of CZTS nanoparticles may be due to different dissolving rates in OLA.¹⁹ Byeon et al.¹⁹ reported that a significant compositional change of CZTS films was observed when the film was annealed above 300 °C, due to some losses of S and Sn. In this work, the reaction temperature of 240 °C was selected because of more uniform nanoparticles' size.

Figure 3 shows the XRD patterns of the CZTS nanoparticles synthesized at different temperatures. The XRD

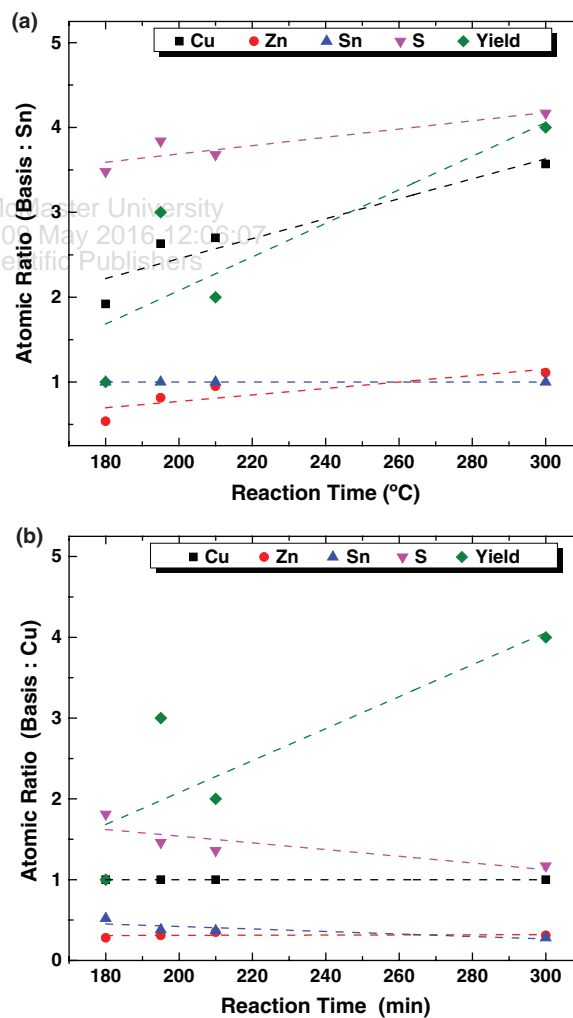


Figure 5. EDS analysis of CZTS nanoparticles synthesized for various times (a) when Sn ratio is fixed to a reference (Sn = 1) and (b) when Cu ratio is fixed to a reference (Cu = 1).

peaks were analyzed and compared with the data of JCPDS card No 26-0575 for tetragonal CZTS (referred as red box ■).²⁰ Other secondary or ternary XRD peaks were referred CuS as empty orange circle (○), Cu₂S as orange dot (●), Cu₂Sn₃S₇ as purple upper triangle (▲), Cu₃SnS₄ as black clover (♣) and Cu₄SnS₄ as left triangle (◄).²¹ All the samples exhibited the strongest peak near $2\theta = 28.5^\circ$, which correspond to (1 1 2) plane of tetragonal CZTS, and several small peaks associated with CZTS phase. In addition, some secondary and ternary phases were observed from the XRD patterns. This may be due to non-stoichiometric composition of Cu rich and S poor, as shown in Figure 3. As the reaction temperature was higher, the intensity of the (1 1 2) plane peak increased, indicating improvement of crystallinity. When the reaction temperature further increased over 300 °C, a strong diffraction peak appeared at $2\theta = 32.1^\circ$, which is related to the secondary SnS phase. The formation of SnS phase is attributed to thermal decomposition of CZTS, as the following reaction,^{17, 19} or abnormal stoichiometry states of Cu rich, Sn and S poor.

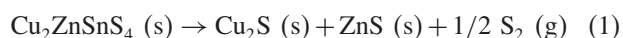


Figure 4 shows the SEM images of the CZTS nanoparticles synthesized for various times. From the figures, the nanoparticles became larger when the reaction time was longer.

Figure 5 shows the EDS analysis of CZTS nanoparticles synthesized for various times. When the reaction time increased, the ratio of Cu and S increased. In particular, the significant deviation from the stoichiometry of CZTS due to higher Cu ratio than 4 was observed for 300 min, compared to the results of the reaction temperature, as shown in Figure 2. This is attributed to smaller chalcogen loss than Sn loss at the reaction temperature of 240 °C, as seen in Figure 5(b).

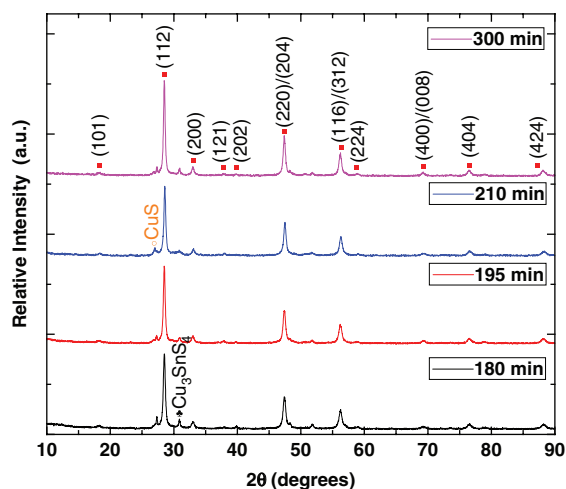


Figure 6. XRD patterns of the CZTS nanoparticles synthesized for various reaction times.

Figure 6 shows the XRD patterns of the CZTS nanoparticles synthesized for various reaction times. The diffraction peaks related to the secondary CuS and ternary Cu₃SnS₄ were observed because of Cu too rich and Sn poor system.²² However, the additional secondary or ternary phases were not formed, although the reaction time increases.

4. CONCLUSION

The effects of synthesis conditions including reaction temperature and time on the properties of the CZTS nanoparticles. As the synthesis temperature and time increased, the nanoparticles became larger. The CZTS nanoparticles with uniform size were obtained at the reaction temperature of 240 °C. In addition, the significant deviation from the stoichiometry of CZTS was observed for longer reaction times. From the XRD analysis, the strongest peak corresponded to (1 1 2) plane of tetragonal CZTS and some peaks associated with secondary and ternary phases were observed, regardless of the synthesis conditions. In particular, a strong diffraction peak appeared corresponded the secondary SnS phase over 300 °C.

Acknowledgment: This work was supported by a grant from the Korea Research Foundation (KRF), funded by the Korean government (MEST) (No. 2012R1A1A2008591). In addition, this work was also supported by the Human Resources Development program (No. 20144030200580) of the Korea Institute of Energy Technology Evaluation and Planning (KETEP) grant funded by the Korean government Ministry of Trade, Industry and Energy.

References and Notes

1. P. Jackson, D. Hariskos, E. Lotter, S. Paetel, R. Wuerz, R. Menner, W. Wischmann, and M. Powalla, *Prog. Photovolt: Res. Appl.* 19, 894 (2011).
2. S. Taunier, J. Sixx-Kurdi, P. P. Grand, A. Chomont, O. Ramdani, L. Parissi, P. Panheleux, N. Naghavi, C. Hubert, M. Ben-Farah, J. P. Fauvarque, J. Connolly, O. Roussel, P. Mogensen, E. Mahé, J. F. Guillemoles, D. Lincot, and O. Kerrec, *Thin Solid Films* 480, 526 (2005).
3. D. Herrmann, P. Kratzert, S. Weeke, M. Zimmer, J. D. Reiss, R. Hunger, P. Lindberg, E. Wallin, O. Lundberg, and L. Stolt, *Proceedings of the 40th IEEE Photovoltaic Specialist Conference (PVSC)*, Denver (2014), p. 2775.
4. G. Yue, D. Lu, B. Cheng, B. Sang, and B.J. Stanbery, *Proceedings of the 40th IEEE Photovoltaic Specialist Conference (PVSC)*, Denver (2014), p. 2056.
5. J. J. Scragg, P. J. Dale, L. M. Peter, G. Zoppi, and I. Forbes, *Phys. Stat. Sol. (b)* 245, 1772 (2008).
6. L. Guen, *J. Sol. Stat. Chem.* 35, 10 (1980).
7. K. Ito and T. Nakazawa, *Jpn. J. Appl. Phys.* 27, 2094 (1988).
8. C. H. Henry, *J. Appl. Phys.* 51, 4494 (1980).
9. K. Tanaka, N. Moritake, and H. Uchiki, *Sol. Energ. Mat. Sol. Cells* 91, 1199 (2007).
10. J. J. Scragg, P. J. Dale, and L. M. Peter, *Jpn. J. Appl. Phys.* 40, 500 (2001).
11. M. A. Contreras, M. J. Romero, B. To, F. Hasoon, R. Noufi, S. Ward, and K. Ramanathan, *Thin Solid Films* 403–404, 204 (2002).

12. B. Shin, O. Gunawan, Y. Zhu, N. A. Bojarczuk, S. J. Chey, and S. Guha, *Prog. Photovolt: Res. Appl.* 21, 72 (2013).
13. W. Wang, M. T. Winkler, O. Gunawan, T. Gokmen, T.K. Todorov, Y. Zhu, and D. B. Mitzi, *Adv. Energy Mater.* 4, 1301465 (2014).
14. C. M. Fella, Y. E. Romanyuk, and A. N. Tiwari, *Sol. Energ. Mat. Sol. Cells* 119, 276 (2013).
15. C. Steinhagen, M. G. Panthani, V. Akhavan, B. Goodfellow, B. Koo, and B. A. Korgel, *J. Am. Chem. Soc.* 131, 12554 (2009).
16. Y. Zou, X. Su, and J. Jiang, *J. Am. Chem. Soc.* 135, 18377 (2013).
17. J. J. Scragg, T. Ericson, T. Kubart, M. Edoff, and C. Platzer-Bjorkman, *Chem. Mater.* 23, 4625 (2011).
18. J. J. Scragg, T. Kubart, J. T. Watjen, T. Ericson, M. K. Linnarsson, and C. Platzer-Bjorkman, *Chem. Mater.* 25, 3162 (2013).
19. M. R. Byeon, E. H. Chung, J. P. Kim, T. E. Hong, J. S. Jin, E. D. Jeong, J. S. Bae, Y. D. Kim, S. Park, W. T. Oh, Y. S. Huh, S. J. Chang, S. B. Lee, I. H. Jung, and J. Hwang, *Thin Solid Films* 546, 387 (2013).
20. X. Lin, J. Kavalakkatt, K. Kornhuber, S. Levchenko, M. C. Lux-Steiner, and A. Ennaoui, *Thin Solid Films* 535, 10 (2013).
21. A.-J. Cheng, M. Manno, A. Khare, C. Leighton, S. A. Campbell, and E. S. Aydil, *J. Vac. Sci. Technol. A* 29, 051203 (2011).
22. I. D. Olekseyuk, I. V. Dudchak, and L. V. Piskach, *J. Alloy. Compd.* 368, 135 (2004).

Received: 17 February 2015. Accepted: 27 May 2015.

Delivered by Ingenta to: McMaster University
IP: 188.72.126.103 On: Mon, 09 May 2016 12:06:07
Copyright: American Scientific Publishers